INORGANIC CHEMISTRY
FRONTIERS

RESEARCH ARTICLE

View Article Online
View Journal | View Issue

Cite this: *Inorg. Chem. Front.*, 2019, **6**, 493

Charge transfer and slow magnetic relaxation in a series of cyano-bridged $Fe^{III}_4M^{II}_2$ (M = Fe^{II}, Co^{II}, Ni^{II}) molecules†

Jin-Hua Wang,[a] Kuduva R. Vignesh,[b] Jia Zhao,[a] Zhao-Yang Li *[a] and Kim R. Dunbar *[b]

Received 17th November 2018,
Accepted 21st December 2018

DOI: 10.1039/c8qi01245h

rsc.li/frontiers-inorganic

The synthesis, single-crystal structures and magnetic properties of three new cyano-bridged complexes $[Fe^{III}_4M^{II}_2]$ (M = Fe^{II}, Co^{II}, Ni^{II}) are reported. Electronic absorption spectroscopy reveals the occurrence of intervalence charge transfer for $[Fe^{III}_4Fe^{II}_2]$. Field-induced slow magnetic relaxation behavior is exhibited for $[Fe^{III}_4Co^{II}_2]$ and $[Fe^{III}_4Ni^{II}_2]$ which originates from the ferromagnetic interactions between Fe^{III} and M^{II} spin centers of the square.

Solid-state molecular materials can potentially be used for sensing and information storage and their development and engineering is of high practical significance.[1–3] Among these materials, some of the most celebrated ones belong to the Prussian blue family derived from cyanometallates, comprising metal ions bridged by cyanide ligands in a linear fashion.[4–6] Over the last several decades, these complexes have attracted a great deal of attention owing to their structural diversity and extraordinary magnetic properties. For example, cyanometallate containing molecules and materials have been reported to exhibit single-molecule magnet (SMM)[7,8] and single-chain magnet (SCM) behavior,[9–11] to undergo spin crossover (SCO)[12–14] and charge transfer–induced spin transitions (CTIST),[15–17] as well as behave as magnetic coolants.[18]

The suitability of cyano-bridged complexes to act as building blocks facilitates the successful exploitation of their unusual technological applications.[19–21] Typically, cyanide ions form linear μ-CN linkages between two metal fragments, which results in moderate to strong magnetic interactions between spin centers and allows for the construction of large molecules and networks.[22,23] Such a modular approach can be used to design new magnetic materials including single molecule magnets. This method has been successfully employed in the exploration of cyano-bridged square-like bimetallic complexes with unusual magnetic behavior.[24] For example, Li and Holms reported an S = 6 octanuclear $[Fe^{III}_4Ni^{II}_4]$ complex exhibiting slow magnetic relaxation,[25] and Oshio and coworkers reported $[Fe^{III}_2Co^{II}_2]$ complexes exhibiting CTIST upon the action of chemical modification and external stimuli.[26] Additionally, the Oshio group reported another cyano-bridged hexanuclear $[Fe^{III}_4Co^{II}_2]$ complex exhibiting an electron transfer–coupled spin transition before light irradiation and featuring slow magnetic relaxation behavior after light irradiation.[27] On the basis of available literature, it can be concluded that, whereas charge transfer in Fe–Co clusters is easily accessible, Fe(III/II) complexes exhibiting charge transfer behavior are rather rare.[28] Moreover, structural distortions and the incorporation of anisotropic metal centers into the molecules could ultimately afford analogues with optimized SMM behavior.

As part of our continuing work on the preparation of new cyano-bridged bimetallic molecules and the pursuit of functional magnetic materials, we have prepared three new heterobimetallic hexanuclear cyano-bridged complexes, $[Fe^{III}_4M^{II}_2]$ (M = Fe^{II}, **1**; Co^{II}, **2**; Ni^{II}, **3**), from TPTZ (2,4,6-tri(pyridin-2-yl)-1,3,5-triazine) and $(NEt_4)[Fe^{III}(Tp^*)(CN)_3]$ (Tp* = tris(3,5-dimethylpyrazol-1-yl)borohydride). Herein, we describe the synthesis, single-crystal structures, and magnetic properties of these compounds, as well as electronic spectral studies that reveal the occurrence of intervalence charge transfer for **1**. Dynamic alternating current (AC) magnetic susceptibility measurements demonstrate that **2** and **3** exhibit field-induced SMM behavior.

Complexes **1–3** were synthesized by reacting $(NEt_4)[Fe^{III}(Tp^*)(CN)_3]$ with $M(ClO_4)_2{\cdot}6H_2O$ (M = Fe^{II}, Co^{II}, Ni^{II}) and TPTZ (2 : 1 : 1 mol/mol/mol) in MeOH : H_2O (2 : 1, v/v). Single-crystal X-ray diffraction (XRD) analyses revealed that **1–3** are isostructural and crystallize as neutral hexanuclear $Fe^{III}_4M^{II}_2$ (M = Fe^{II}, Co^{II}, Ni^{II}) species in the triclinic space group. The asymmetric unit of **1–3** contains two unique Fe^{III} centers, one

[a]*School of Materials Science and Engineering, Nankai University, Tianjin 300350, China. E-mail: zhaoyang@nankai.edu.cn*
[b]*Department of Chemistry, Texas A&M University, College Station, Texas 77842-3012, USA. E-mail: dunbar@chem.tamu.edu*

†Electronic supplementary information (ESI) available. CCDC 1840682, 1840679 and 1840680. For ESI and crystallographic data in CIF or other electronic format see DOI: 10.1039/c8qi01245h

TPTZ ligand, and one unique M^{II} center. The central square core ($[Fe_2^{III}M_2^{II}]^{2+}$) features $[Fe(\mu\text{-}CN)_2(CN)(Tp^*)]^-$ and $[M(TPTZ)]^{2+}$ units bridged by cyanide ligands, with two additional $[Fe(\mu\text{-}CN)(CN)_2(Tp^*)]^-$ units linked to the M^{II} ions of the square to form the overall hexanuclear compound. In the square core, each M^{II} ion is coordinated to one TPTZ ligand and three cyanide carbon atoms in a slightly distorted octahedral coordination environment (Fig. 1 and Fig. S1 and S4†).

In the tetranuclear unit $[Fe_2^{III}(\mu\text{-}CN)_4M_2^{II}]$ the M^{II}–N≡C bond angles are ~180° (174.3(3)–178.9(3)° for **1**, 172.0(3)–177.9(3)° for **2**, and 173.13(16)–179.2(2)° for **3**) which facilitates the formation of nearly almost planar structure. The Fe^{III}–C≡N bond angles (166.4(2)–170.9(2)° for **1**, 150.3(2)–172.3(3)° for **2**, and 155.66(15)–174.27(15)° for **3**), however, exhibit significant deviations from 180°, and a deviation from planarity for the two $[(Tp^*)Fe^{III}(CN)_3]_2$ groups (Fig. S1c, S4c and S7b†). The Fe^{III}–C bond distances in **1–3** are 1.904(3)–1.938(3), 1.903(3)–1.940(3), and 1.903(2)–1.932(2) Å, respectively, and are close to values reported for other Tp* complexes, indicating that all three Fe^{III} ions are low-spin.[29] The average M^{II}–$N_{cyanide}$ bond distances in **1–3** are 2.119, 2.075 and 2.039 Å, respectively.

The packing arrangements of complexes **1–3** involves weak intermolecular interactions between the $[Fe_4^{III}M_2^{II}]$ molecules. In the case of **1**, these interactions involve (a) the carbon atoms of TPTZ and the nitrogen atoms of Tp* in another adjacent $[Fe_4^{III}Fe_2^{II}]$ cluster to form a C47–H47···N3 (3.449 Å) hydrogen bond, (b) the carbon atoms of TPTZ and the nitrogen atoms of uncoordinated cyanide ions in $[Fe(\mu\text{-}CN)(CN)_2(Tp^*)]^-$ units to form a C39–H39···N7 (3.268 Å) hydrogen bond, and (c) the carbon atoms of $[Fe(\mu\text{-}CN)(CN)_2(Tp^*)]^-$ units and the nitrogen atoms of TPTZ to form a C29–H29B···N24 (3.533 Å) hydrogen bond to yield 2D supramolecular layers. In addition to intermolecular hydrogen bonds, two types of C–H···π interactions are present, namely those between the carbon atom of TPTZ and the pyrazole ring of $[Fe(\mu\text{-}CN)(CN)_2(Tp^*)]^-$ units (C46–H46···$Cg_{N1–N2–C32–C31–C30}$ and C47–H47···$Cg_{N3–N4–C22–C21–C20}$ distances of 3.587 and 3.430 Å, respectively). There are also π···π interactions between the rigid tridentate TPTZ ligands of two adjacent $[Fe_4^{III}Fe_2^{II}]$ units (Fig. S2 and S3†). Finally, weak interactions between molecules were also observed in complexes **2** and **3** which lead to the stabilization of a 3D supramolecular architecture (Fig. S5–S7†).

To confirm the phase purity of these three complexes, the PXRD patterns were recorded. The presented results show that most of the peak positions of the simulated and experimental patterns are in good agreement with each other (Fig. S8–S10†). Thermogravimetric analysis (TGA) was carried out to study the stability of the coordination architectures of complexes **1–3** under air atmosphere with a heating rate of 10 °C min^{-1} (Fig. S11–S13†).

Fig. 2 displays the UV-visible absorption spectra of **1–3**, TPTZ, and $(NEt_4)[Fe^{III}(Tp^*)(CN)_3]$ recorded in MeOH at room temperature. There are three absorption maxima (207, 248, and 285 nm) in the case of TPTZ and two features (210 and 445 nm) in the case of $(NEt_4)[Fe^{III}(Tp^*)(CN)_3]$. Notably, the spectrum of **2** resembles that of **3**, whereas the spectrum of **1** exhibits a characteristic absorption peak at 590 nm that is assigned to intervalence charge transfer (IVCT) between Fe(II) and Fe(III).[30] To the best of our knowledge, **1** is the first cyano-bridged square complex that exhibits IVCT between Fe(II) and Fe(III).

Magnetic measurements were performed on crushed polycrystalline samples of **1–3** using a SQUID magnetometer. The dependence of χT *versus* T was determined for **1–3** from 300–1.8 K (Fig. S14, S15† and Fig. 3). The χT value is 7.2 emu K mol^{-1} for **1** at 300 K, which is closed to the spin-only value (7.5 emu K mol^{-1}) for the $[Fe_4^{III}Fe_2^{II}]$ unit ($S_{Fe(III)} = 1/2$, $S_{Fe(II)} = 2$, $g = 2.0$). The χT value is 8.5 emu K mol^{-1} for **2** at 300 K, which is much higher than the spin-only value (5.25 emu K mol^{-1}) for the $[Fe_4^{III}Co_2^{II}]$ unit ($S_{Fe(III)} = 1/2$, $S_{Co(II)} = 3/2$, $g = 2.0$), an indication of strong spin–orbit coupling effects.[31] The χT value for **3** at 300 K is 3.46 emu K mol^{-1} which is close to the expected spin-only value (3.5 emu K mol^{-1}) for the $[Fe_4^{III}Ni_2^{II}]$ unit ($S_{Fe(III)} = 1/2$, $S_{Ni(II)} = 1$, $g = 2.0$). The values of χT gradually increase with decreasing temperature, reaching a maximum of 11.8 emu K mol^{-1} for **2** and 14.3 emu K mol^{-1} for **3** at 4 K,

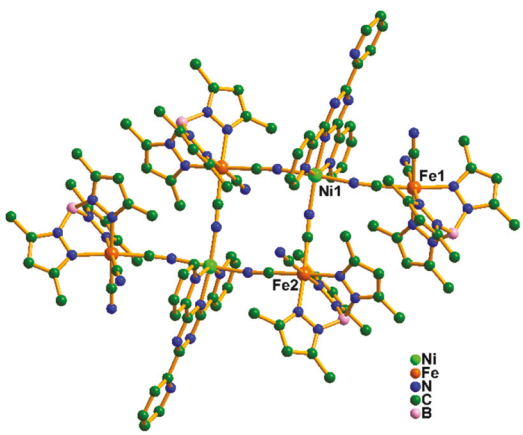

Fig. 1 Single-crystal structure of **3** (solvent molecules and H atoms are omitted for clarity).

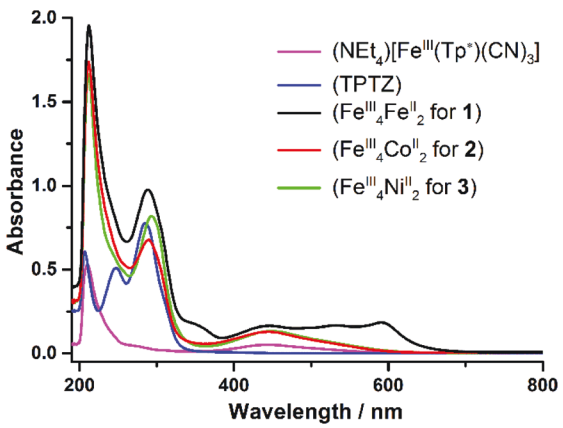

Fig. 2 UV-vis absorption spectra of **1–3** measured in MeOH at room temperature.

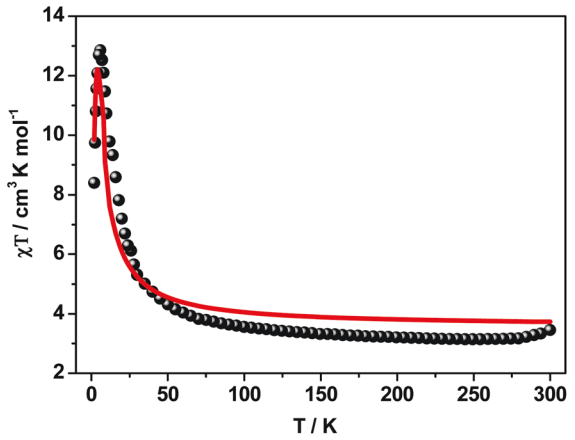

Fig. 3 Magnetic susceptibility of **3** (χT) plotted *versus* temperature (K). The solid lines correspond to the fitting results.

indicative of weak ferromagnetic coupling between M^{II} and Fe^{III} spin centers in these complexes. Upon further cooling to $T < 4$ K, χT abruptly decreases to a minimum of 9.4 emu K mol^{-1} for **2** and 13.1 emu K mol^{-1} for **3** at 1.8 K, which is ascribed to zero-field splitting, and/or weak interactions.

In order to extract the nature and the magnitude of the spin Hamiltonian parameters (J, g and D) within each complex, we performed the fitting of the experimental magnetic data by using PHI program.[32] To avoid over parameterization only two magnetic exchange parameter values (J_1 and J_2 (see Fig. S16†)) are considered due to the complications of performing fits of experimental data with multiple J's. The M^{II}–Fe^{III} magnetic interactions within the central square core $[Fe^{III}_2M^{II}_2]$ were considered as J_1 and the interactions of M^{II} ions with the outer Fe^{III} ions were considered as J_2. The results of fitting the magnetic data are presented in Table 1. Eqn (1) is the Hamiltonian used to fit the magnetic data to determine J's, and g and D values of M(II) centers for each complex (g value of LS–Fe(III) centers were fixed as 2.0).

$$\hat{H} = -[2J_1(S_{M1}S_{Fe2} + S_{M1}S_{Fe2'} + S_{M1'}S_{Fe2} + S_{M1'}S_{Fe2'}) + 2J_2(S_{M1}S_{Fe1} + S_{M1'}S_{Fe1'})] + DSz^2 + g\beta H\cdot S \quad (1)$$

From the extracted values it's indicative that the four possible J_1 magnetic interactions are dominant interactions that supports the overall χT profiles as ferromagnetic nature for **2** and **3** and antiferromagnetic nature for **1**. The two possible J_2 values are opposite sign to the J_1 and they do not play a role in deciding the χT profiles nature owing to their smaller magnitude in **1** and **2**. Whereas in **3**, the J_2 values also ferromagnetic in nature supports the presence of strong ferromagnetic behavior with considering small intermolecular interactions (zJ = 0.03). The extracted g values of M^{II} centers supports their spin–orbit coupling nature. The extracted positive D values suggesting the low temperature magnetic behavior.

To probe the magnetic anisotropy of **3**, the magnetization M (μ_B) data were plotted against the external magnetic field H (T) at different low temperatures. The resulting magnetization plots are non-superimposable with the significant separations between the isotherm curves being indicative of strong magnetic anisotropy. The magnetization data are nearly saturated at 7 T, approaching a maximum value of 4.5μ_B over a series of temperature ranges (Fig. S18†).

Dynamic AC measurements revealed that **2** and **3**, in contrast to **1**, exhibit slow magnetic relaxation behavior. In particular, the temperature and frequency dependence of in-phase (χ') and out-of-phase (χ'') AC magnetic susceptibilities demonstrated that **3** shows typical SMM behavior, which was further probed by determining the temperature and frequency dependences of χ' and χ'' under various direct current (DC) magnetic fields (0, 300, 600, 900, and 1200 Oe; Fig. S19, S20, Fig. 4, S21, and S22,† respectively). The best results were obtained at a DC field of 600 Oe, which indicates that the QTM effect is sufficiently suppressed by DC fields. As illustrated in Fig. 4, both χ' and χ'' exhibit a characteristic dependence on frequency under a DC field of 600 Oe, namely as the temperature is increased from 1.8 to 2.5 K, the intensity of the χ'' peak slightly decreases, and the peak shifts to higher frequencies. The magnetic relaxation processes were further examined by using the Debye model to construct Cole–Cole plots based on AC magnetic susceptibility data obtained under a 600 Oe DC field, as shown in Fig. 5. The effective energy barrier and relaxation time (τ) were extracted from Arrhenius plots of $\ln(t)$ *vs.* T^{-1} and are 16.16 cm^{-1} and 1.0 × 10^{-8} s for **3** (Fig. S24†), which are in the similar range of reported Ni(II)-based SMMs.[34,35]

Table 1 Experimentally fitted J values (in cm^{-1}), and g and D (in cm^{-1}) values of M(II) centers of complexes **1–3**. The ZFS parameter D of 36.2 cm^{-1} appears slightly large by comparison to the values usually reported for related Fe(II) complexes[33]

$Fe^{III}_4M^{II}_2$	J_1	J_2	g	D
M = Fe(II) (**1**)	−10.3	+2.2	2.06	+36.2
M = Co(II) (**2**)	+2.7	−1.1	2.64	+3.9
M = Ni(II) (**3**)	+5.1	+5.0	2.26	+8.6

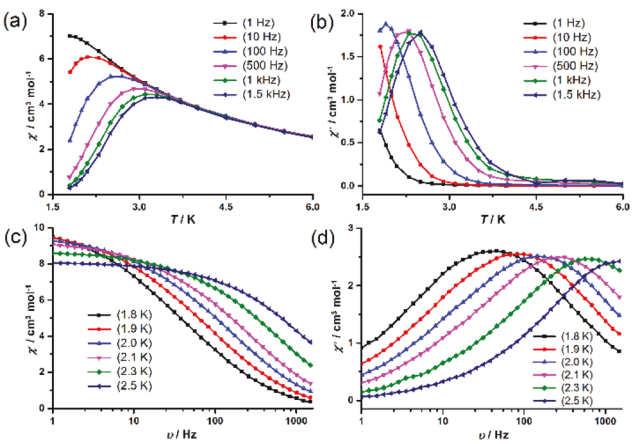

Fig. 4 Temperature and frequency dependences of χ' and χ'' in a 600 Oe DC field determined for **3** at AC frequencies of 1–1500 Hz.

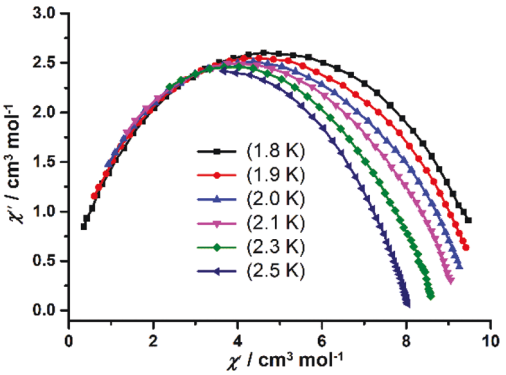

Fig. 5 Cole–Cole plots based on the AC susceptibilities of **3** in a 600 Oe DC field between 1.8 and 2.5 K.

In summary, we have described the preparation, single-crystal structures, electronic absorption spectra, and magnetic properties of three new isostructural cyano-bridged hexanuclear $[Fe^{III}_4M^{II}_2]$ (M = Fe^{II}, Co^{II}, Ni^{II}) complexes. The results of the UV-visible spectroscopy studies indicate that the $[Fe^{III}_4Fe^{II}_2]$ molecule exhibits IVCT. Dynamic AC magnetic susceptibility measurements revealed that $[Fe^{III}_4Co^{II}_2]$ and $[Fe^{III}_4Ni^{II}_2]$ exhibit field-induced SMM behavior, which is more pronounced for the latter molecule owing to stronger ferromagnetic interactions.

Conflicts of interest

There are no conflicts of interest to declare.

Acknowledgements

Z. Y. Li thanks Nankai University for start-up funds for young talented researchers. Additionally, this work was supported by the National Natural Science Foundation of China (NSFC, 21701088) and the Natural Science Foundation of Tianjin City (17JCYBJC41000). KRD gratefully acknowledges the National Science Foundation (CHE-1808779) and the Robert A. Welch Foundation (A-1449) for support of this work.

Notes and references

1 J. L. Liu, Y. C. Chen and M. L. Tong, *Chem. Soc. Rev.*, 2018, **47**, 2431–2453.
2 Y. F. Zeng, X. Hu, F. C. Liu and X. H. Bu, *Chem. Soc. Rev.*, 2009, **38**, 469–480.
3 B. S. Dolinar, S. Gomez-Coca, D. I. Alexandropoulos and K. R. Dunbar, *Chem. Commun.*, 2017, **53**, 2283–2286.
4 H. Zheng, Y. S. Meng, G. L. Zhou, C. Y. Duan, O. Sato, S. Hayami, Y. Luo and T. Liu, *Angew. Chem., Int. Ed.*, 2018, **57**, 8468–8472.
5 Y. Z. Zhang, P. Ferko, D. Siretanu, R. Ababei, N. P. Rath, M. J. Shaw, R. Clerac, C. Mathoniere and S. M. Holmes, *J. Am. Chem. Soc.*, 2014, **136**, 16854–16864.
6 D. Q. Wu, D. Shao, X. Q. Wei, F. X. Shen, L. Shi, D. Kempe, Y. Z. Zhang, K. R. Dunbar and X. Y. Wang, *J. Am. Chem. Soc.*, 2017, **139**, 11714–11717.
7 D. Pinkowicz, H. I. Southerland, C. Avendaño, A. Prosvirin, C. Sanders, W. Wernsdorfer, K. S. Pedersen, J. Dreiser, R. Clérac, J. Nehrkorn, G. G. Simeoni, A. Schnegg, K. Holldack and K. R. Dunbar, *J. Am. Chem. Soc.*, 2015, **137**, 14406–14422.
8 K. Qian, X. C. Huang, C. Zhou, X. Z. You, X. Y. Wang and K. R. Dunbar, *J. Am. Chem. Soc.*, 2013, **135**, 13302–13305.
9 V. D. Sasnovskaya, V. A. Kopotkov, A. D. Talantsev, R. B. Morgunov, E. B. Yagubskii, S. V. Simonov, L. V. Zorina and V. S. Mironov, *Inorg. Chem.*, 2017, **56**, 8926–8943.
10 C. Pichon, N. Suaud, C. Duhayon, N. Guihery and J. P. Sutter, *J. Am. Chem. Soc.*, 2018, **140**, 7698–7704.
11 L. Su, W. C. Song, J. P. Zhao and F. C. Liu, *Chem. Commun.*, 2016, **52**, 8722–8725.
12 R. M. Wei, M. Kong, F. Cao, J. Li, T. C. Pu, L. Yang, X. L. Zhang and Y. Song, *Dalton Trans.*, 2016, **45**, 18643–18652.
13 O. I. Kucheriv, S. I. Shylin, V. Ksenofontov, S. Dechert, M. Haukka, I. O. Fritsky and I. y. A. Gural'skiy, *Inorg. Chem.*, 2016, **55**, 4906–4914.
14 C. Y. Zheng, J. P. Xu, F. Wang, J. Tao and D. F. Li, *Dalton Trans.*, 2016, **45**, 17254–17263.
15 L. Cao, J. Tao, Q. Gao, T. Liu, Z. C. Xia and D. F. Li, *Chem. Commun.*, 2014, **50**, 1665–1667.
16 J. X. Hu, L. Luo, X. J. Lv, L. Liu, Q. Liu, Y. K. Yang, C. Y. Duan, Y. Luo and T. Liu, *Angew. Chem., Int. Ed.*, 2017, **56**, 7663–7668.
17 J. M. Zadrozny, D. E. Freedman, D. M. Jenkins, T. D. Harris, A. T. Iavarone, C. Mathoniere, R. Clerac and J. R. Long, *Inorg. Chem.*, 2010, **49**, 8886–8896.
18 P. Konieczny, L. Michalski, R. Podgajny, S. Chorazy, R. Pelka, D. Czernia, S. Buda, J. Mlynarski, B. Sieklucka and T. Wasiutynski, *Inorg. Chem.*, 2017, **56**, 2777–2783.
19 E. V. Alexandrov, A. V. Virovets, V. A. Blatov and E. V. Peresypkina, *Chem. Rev.*, 2015, **115**, 12286–12319.
20 J. X. Hu, Y. Xu, Y. S. Meng, L. Zhao, S. Hayami, O. Sato and T. Liu, *Angew. Chem., Int. Ed.*, 2017, **56**, 13052–13055.
21 L. Alcázar, G. Aullón, M. Ferrer and M. Martínez, *Chem. – Eur. J.*, 2016, **22**, 15227–15230.
22 A. S. Sergeenko, J. S. Ovens and D. B. Leznoff, *Chem. Commun.*, 2018, **54**, 1599–1602.
23 D. Shao, Y. Zhou, Q. Pi, F. X. Shen, S.-R. Yang, S. L. Zhang and X. Y. Wang, *Dalton Trans.*, 2017, **46**, 9088–9096.
24 C. Y. Zheng, J. P. Xu, Z. X. Yang, J. Tao and D. F. Li, *Inorg. Chem.*, 2015, **54**, 9687–9689.
25 D. F. Li, S. Parkin, G. B. Wang, G. T. Yee, R. Clérac, W. Wernsdorfer and S. M. Holmes, *J. Am. Chem. Soc.*, 2006, **128**, 4214–4215.
26 M. Nihei, Y. Sekine, N. Suganami, K. Nakazawa, A. Nakao, H. Nakao, Y. Murakami and H. Oshio, *J. Am. Chem. Soc.*, 2011, **133**, 3592–3600.

27 M. Nihei, Y. Okamoto, Y. Sekine, N. Hoshino, T. Shiga, I. P. Liu and H. Oshio, *Angew. Chem., Int. Ed.*, 2012, **51**, 6361–6364.
28 K. R. Zhang, K. Soonchul, Z. S. Yao, N. Kazusa, Y. Takashi, E. Yasuaki, A. Nobuaki, M. Yuji, N. Motohiro, K. Shinji and S. Osamu, *Angew. Chem., Int. Ed.*, 2016, **55**, 6047–6050.
29 D. F. Li, S. Parkin, G. B. Wang, G. T. Yee, A. V. Prosvirin and S. M. Holmes, *Inorg. Chem.*, 2005, **44**, 4903–4905.
30 M. Nihei, M. Ui, N. Hoshino and H. Oshio, *Inorg. Chem.*, 2008, **47**, 6106–6108.
31 Y. Z. Zhang, S. Gomez-Coca, A. J. Brown, M. R. Saber, X. Zhang and K. R. Dunbar, *Chem. Sci.*, 2016, **7**, 6519–6527.
32 N. F. Chilton, R. P. Anderson, L. D. Turner, A. Soncini and K. S. Murray, *J. Comput. Chem.*, 2013, **34**, 1164–1175.
33 C. Pichon, N. Suaud, C. Duhayon, N. Guihery and J. P. Sutter, *J. Am. Chem. Soc.*, 2018, **140**, 7698–7704.
34 D. F. Li, R. Clérac, S. Parkin, G. B. Wang, G. T. Yee and S. M. Holmes, *Inorg. Chem.*, 2006, **45**, 5251–5253.
35 D. F. Li, S. Parkin, G. B. Wang, G. T. Yee, R. Clérac, W. Wernsdorfer and S. M. Holmes, *J. Am. Chem. Soc.*, 2006, **128**, 4214–4215.